THEORETICAL CHARACTERIZATION OF POLYMER-BLEND BULK HETEROJUNCTION ORGANIC SOLAR CELLS

Ana Bărar[1], Marian Vlădescu[2], Paul Şchiopu[3]

The theoretical characterization of several poly(3-hexylthiophene) (P3HT) based organic solar cells, with novel donor polymers, was realised by calculating the internal parameters associated to the equivalent model for an organic solar cell, and by using the cells' respective J-U characteristics and the Lambert W function. The following parameters were extracted: fill-factor, power conversion efficiency, series resistance, shunt resistance, and ideality factor. In terms of fill-factor and efficiency, among the samples which were studied here, the highest performing prototype is a $P(4)$*-*$T4-SiDT:PC_{71}BM(1:1)$ *+* $2\%DIO$ *on* MoO_3*;* Ca/Al *polymer blend prototype, according to the fill-factor* $FF = 0.62$ *and efficiency* $PCE = 4.9\%$ *that were obtained. Regarding this particular probe, a further study was led on the variation of its efficiency with the width of the active layer, which concluded with determining an optimal width* $L = 500$ *nm, for which a peak efficiency* $PCE = 5.11\%$ *was obtained.*

Keywords: photovoltaic cell, organic semiconductors, polymer blends, W Lambert function

1. Introduction

During the last decades, intensive research has been conducted in the field of materials science to study the electric and electro-optic properties of functional materials in conjunction with liquid crystals [1–8]. Among these materials, the electric and electro-optic of different types of polymers [9–15], carbon nanotubes (CNT-s) and nanorods (CNR-s) [15–19] have been extensively studied. While solar cells enhanced with such materials exhibit qualitatively improved properties, the requirement of special conditions (heat treatment, infrared filtering etc.), together with an expensive manufacturing process still make them an unlikely candidate for large-scale implementation. An alternative for inorganic solar cells in the low-power applications regime is the use of bulk organic solar cells, due to certain advantages: their cost-effective and non-pretentious fabrication technology, together their high mechanical flexibility renders them appropriate for a wide range of applications [20]. Also, the bulk structure can be enhanced by chemically engineered semiconducting polymers, resulting in improved properties [21]. However, organic solar cells have one major drawback, their low power conversion efficiency, compared to inorganic devices [22]. In order to better understand what factors cause poor power conversion efficiency

[1]Assisting Lecturer, Department of Electronic Technology and Reliability, University "Politehnica" of Bucharest, Romania, e-mail: ana.barar@yahoo.ro

[2]Associate Professor, Department of Electronic Technology and Reliability, University "Politehnica" of Bucharest, Romania

[3]Professor, Department of Electronic Technology and Reliability, University "Politehnica" of Bucharest, Romania

in organic solar cells, a thorough study of their working parameters and their dependency to semiconducting polymer properties is necessary.

This paper focuses mainly on the bulk heterojunction structure (BHJ). It consists of a heterogenous blend between an acceptor semiconducting polymer and a donor one, spread in a thin layer, called an active layer. The active layer is sandwiched between two electrodes: one electrode must be transparent, in order to allow the absorption of incident light by the active layer, while the second electrode is generally a metallic substrate. This architecture is illustrated in Figure 1.

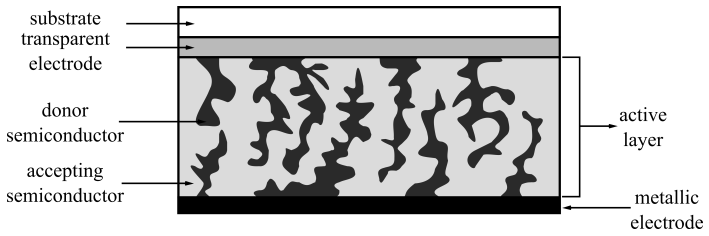

FIGURE 1. Basic structure of a bulk heterojunction solar cell [25]

For characterization purposes, several organic solar cells built by following this architecture have been selected from literature [23]. These prototypes contain standard fullerene-based acceptor polymers associated with novel donor polymers, and a few of them also have anode buffer layers. The purpose of this paper is to characterize these solar cells, by extracting their internal parameters, with the use of their equivalent physical model and their respective current-voltage characteristics. The determination was carried out on data provided by reference [23] by two separate methods: an asymptotic calculation, which provides a rough estimate, and a Lambert W function procedure, which uses the rough estimates obtained in the asymptotic calculations as its input, in order to achieve greater accuracy [26]. Furthermore, based on the values obtained for the parameters, the device with the best performance has been selected, and the variation of its efficiency with the width of the active layer has been studied.

2. **Equivalent physical model**

The most frequently used physical model for a solar cell consists of a diode D, representing the p-n junction of the cell, a current source J_L, which corresponds to the illumination current density, a shunt resistance R_p, which models defects both at the surface and in the bulk of the active layer, and a series resistance R_s, associated to the metal contacts of the device [28, 29]. The model is presented in Figure 2.

The illumination current density J_L is defined by the following relation [28, 29]:

$$J_L = eG\mu\tau\left(\frac{U_{bi}-U}{L}\right)\left[1-\exp\left(-\frac{L^2}{\mu\tau\,(U_{bi}-U)}\right)\right] \tag{1}$$

where e is the elementary charge of an electron, G represents the charge carrier generation rate, U_{bi} is the bias voltage, U is the load voltage, L is the thickness of the photo-active layer, and $\mu\tau$ is the product between the charge carrier mobility μ, and their τ. The current density J_j through the diode D is defined by the following relation [28]:

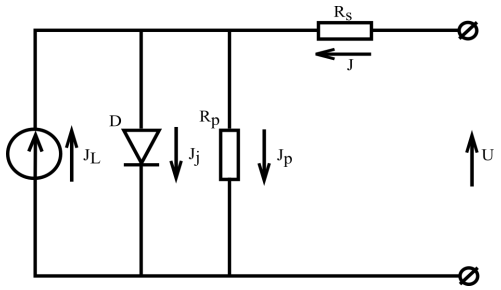

FIGURE 2. One-diode model of an organic solar cell [28]

$$J_j = J_s \left[\exp \left[e \frac{U - R_s J}{\gamma k_B T} \right] - 1 \right] \tag{2}$$

where k_B is the Boltzmann constant, J is the total current density, T is the absolute temperature of the diode, J_s is the dark saturation current density, and γ is the ideality factor.

The current density J_p running through the shunt resistance R_p has the following form [28]:

$$J_p = \frac{U - R_s J}{R_p} \tag{3}$$

By applying the Kirchhoff laws to the model presented in Figure 1, and through further calculations, the equation for the total current density J is obtained [28]:

$$J = J_s \left[\exp \left[e \frac{(U - R_s J)}{\gamma k_B T} \right] - 1 \right] + \frac{U - R_s J}{R_p} - J_L \tag{4}$$

The aim of the following calculations is to determine the physical measures R_s, γ, R_p and J_s from equation (4), for several organic solar cells,selected from the state-of-the-art. Since relation (4) is a transcendental equation, numerical methods had to be considered for its solving. As discussed in [26, 29, 33], the Lambert W function is a reliable bypass method, which provides precise solutions. A rough estimate of these parameters' values will be obtained with the asymptotic approximation method, and the values will be used as seeds for the Lambert W function.

3. **Asymptotic approximation and the Lambert W function**

The approximation method is a mathematical approach to bypass transcendental equation 4. This method was devised by del Pozo [29], and is detailed in this section. The main idea is to simplify equation 4, in order to obtain parameters R_p, R_s, γ, and J_s, respectively [29–31]. The first approximation is made by eliminating the illumination current density J_L, simplifying equation 4 to the following form:

$$J = J_s \left[\exp \left(e \frac{(U - R_s J)}{\gamma K_B T} \right) - 1 \right] + \frac{U - R_s J}{R_p} \tag{5}$$

Series resistance R_s and ideality factor γ are obtained by considering the current density J_j as being far greater than the current density J_p $(J_j >> J_p)$. This simplification is applied to equation 5, leading to the following form:

$$J = J_s \left[\exp\left(e\frac{(U - R_s J)}{\gamma K_B T} \right) - 1 \right] \tag{6}$$

With further calculations, relation 6 can be rewritten as a function of current density J, as follows:

$$J\frac{dU}{dJ} = R_s J + \frac{\gamma k_B T}{e} \tag{7}$$

Relation 7 corresponds to the short-circuit region of the current-voltage characteristic (see Figure 3), where parameters γ and R_s are determined.

On the other hand, the shunt resistance R_p is obtained by considering that $J_j << J_p$. By applying this simplification to equation 5, the following relation is obtained:

$$J = \frac{U - R_s J}{R_p} \tag{8}$$

By considering that R_p is far greater than R_s, and by adding a few rearrangements to equation 8, the following function is obtained:

$$\frac{dU}{dJ} = R_p \tag{9}$$

Function 9 corresponds to the open-circuit region of the current-voltage characteristic (see Figure 3), where the shunt resistance R_p is determined.

In order to determine J_s, equation 4 is approximated by considering short-circuit conditions ($J = J_{sc}$, $U = 0V$), and by assuming that the illumination current density is equal to the short-circuit current density $J_L = -J_{sc}$. With further rearrangements, the following relation defining J_s is obtained:

$$J_s = \frac{J_{sc}\frac{R_s}{R_p}}{\exp\left(-\frac{eR_s J_{sc}}{\gamma k_B T}\right) - 1} \tag{10}$$

The value of the short-circuit current density J_{sc} is determined from the intersection of the J-U characteristic with the J-axis.

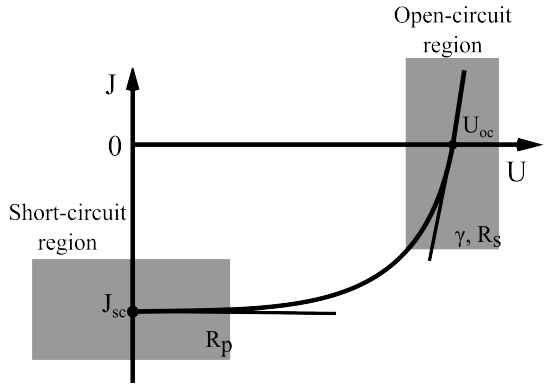

FIGURE 3. Model of the organic photovoltaic cell sample, highlighting the open- and short-circuit [27, 29]

The Lambert W function is mathematically defined as [32]:

$$z = W(z)\exp(W(z)) \tag{11}$$

where $z \in C$. Among its many applications, this function is also used for solving transcendental equations or algorithm analysis [32–34]. The Lambert W function is used here in order to obtain an analytic dependency between the voltage U and the total current density J, based on equation (4). To do this, equation (4) must be rearranged in the following form [32]:

$$X = Y\exp(Y) \leftrightarrow Y = W(X) \tag{12}$$

where Y is a function that depends on J. After a few calculations, equation (4) can reach the following form:

$$\left[\frac{eR_sJ}{\gamma k_BT} + \frac{eR_sR_p\left(J_s + J_L - \frac{U}{R_p}\right)}{\gamma k_BT(R_s+R_p)}\right]\exp\left[\frac{eR_sJ}{\gamma k_BT} + \frac{eR_sR_p\left(J_s + J_L - \frac{U}{R_p}\right)}{\gamma k_BT(R_s+R_p)}\right] = \frac{eR_sR_pJ_s}{\gamma k_BT(R_s+R_p)}\exp\left[\frac{eR_p(U+R_sJ_s+R_sJ_L)}{\gamma k_BT(R_s+R_p)}\right] \tag{13}$$

Equation (13) corresponds to the form presented in (12). Therefore, W can be applied on both sides of equation (13):

$$\left[\frac{eR_sJ}{\gamma k_BT} + \frac{eR_sR_p\left(J_s + J_L - \frac{U}{R_p}\right)}{\gamma k_BT(R_s+R_p)}\right] = W\left[\frac{eR_sR_pJ_s}{\gamma k_BT(R_s+R_p)}\exp\left[\frac{eR_p(U+R_sJ_s+R_sJ_L)}{\gamma k_BT(R_s+R_p)}\right]\right] \tag{14}$$

After a few rearrangements brought to equation (14), the following analytic form is obtained for total current density J. This mathematical model is similar to the one presented by Jain et al. [33]:

$$J = \frac{W\left[\frac{e}{\gamma k_BT}\frac{R_sR_pJ_s}{(R_s+R_p)}\exp\left[\frac{e}{\gamma k_BT}\frac{R_p(U+R_sJ_s+R_sJ_L)}{(R_s+R_p)}\right]\right]}{\frac{e}{\gamma k_BT}R_s} - \frac{R_p}{(R_s+R_p)}\left(J_s + J_L - \frac{U}{R_p}\right) \tag{15}$$

We will show that, when provided with appropriate inputs, the Lambert W function offers a more accurate approximation of the current-voltage characteristic, and therefore, of the circuit parameters.

4. **Polymer blends descriptions**

The donor-acceptor polymer active blends have been deposited as layers on the electrode surface through spin-casting, afterwards, being either thermally annealed or left as-cast. The entire process, as well as the composition of the polymer blends, are explained in detail in [23]: The donor polymers were all designed starting from a dithieno $[3,2-b : 2',3'-d]$ -silole (SiDT) base, which contains an electron rich silicon (Si) atom, thus allowing attachment of several other polymer branches . The SiDT base was associated to

either a dithiophene (2T), or a tetrathiophene (4T) monomer, which provides the polymer with good self-assembly properties and the ability to form highly structured films when being deposited from solution. Finally, polymer radicals $P(1)$, $P(2)$, $P(3)$ and $P(4)$ were added. As acceptor polymers, $[6,6]$ phenyl-C_{61}-butyric acid methyl esther (PC_{61} - BM) and $[6,6]phenyl-C_{71}-butyric\ acid\ methyl\ esther$ $(PC_{71}BM)$ were used. Since $PC_{71}BM$ presents poor miscibility with solvents [35] and, therefore, leads to formation of defects in active layer which could affect the performance of the cell, several cell prototypes were optimized by adding $1,8-diiodooctane$ (DiO), a processing solvent additive. This additive improves the self-organisation properties of the blend, leading to improved layer morphologies. Other methods of cell performance improvement, such as anode and cathode buffer layers depositions, were also tested. The method entails a thin layer of molybdenum oxide (MoO_3) deposited on the anode, and a layer of Ca/Al deposited on the cathode.

5. **Results and Discussions**

To increase the accuracy of the determined values for the different organic solar cells, the experimental data extracted from literature was fitted in the following scheme: First, the data was fitted with two straight lines in the open- and short-circuit regions, and the initial rough values of the circuit parameters have been extracted. Using these initial estimates, the current-voltage characteristic was plotted. Secondly, with the values extracted from the asymptotic approach serving as inputs, the Lambert W function was applied in an iterative manner, and plotted next to the data. The results are shown in Figure 4. The rough estimates of the model parameters are presented in Table 2, and the results obtained with the W Lambert function are presented in Table 3. According to these values, namely the ones obtained for the fill-factor and the power conversion efficiency, the optimal prototype is the one based on $P(4)$-$T4-SiDT:PC_{71}BM(1:1)+2\%DIO$ on MoO_3; Ca/Al polymer blend, for which a fill-factor $FF=0.62$, and an efficiency $PCE=4.9\%$ were obtained. Therefore, this particular polymer was submitted to further studies, namely the variation of the power conversion efficiency PCE of the device with the width L of its active layer. As shown in Figure 5b, a maximum for the power conversion efficiency $PCE=5.11\%$ has been obtained for an active layer width $L=500\ nm$.

TABLE 1. Polymer blends nomenclatures and the associated codes used in this paper

Polymer	Polymer code
$P(3)-T4-SiDT:PC_{61}BM(1:1)$	P1
$P(3)-T4-SiDT:PC_{71}BM(1:1)$	P2
$P(3)-T4-SiDT:PC_{71}BM(1:1)+2\%DIO$	P3
$P(3)-T4-SiDT:PC_{71}BM(1:1)+2\%DIOonMoO_3$	P4
$P(3)-T4-SiDT:PC_{71}BM(1:1)+2\%DIOonMoO_3;Ca/Al$	P5
$P(4)-T4-SiDT:PC_{71}BM(1:1)+2\%DIO$	P6
$P(4)-T4-SiDT:PC_{71}BM(1:1)+2\%DIOonMoO_3$	P7
$P(4)-T4-SiDT:PC_{71}BM(1:1)+2\%DIOonMoO_3;Ca/Al$	P8

TABLE 2. Values obtained for parameters R_s, R_p, γ, J_s, open-circuit voltage U_{oc}, short-circuit current density J_{sc}, fill-factor FF, and power conversion efficiency PCE, with the approximation method

Polymer code	$U_{oc}\,(V)$	$J_{sc}\,(mA/cm^2)$	$R_s\,(\Omega/cm^2)$	$R_p\,(\Omega/cm^2)$	γ	$J_s\,(nA/cm^2)$	FF	$PCE\,(\%)$
P1	0.87	7.08	50.25	763.35	1.08	1.26	0.56	3.5
P2	0.9	4.50	105.20	1181.66	1.29	0.25	0.10	0.4
P3	0.84	8.05	53.02	800.00	1.66	24.10	0.59	4.0
P4	0.82	8.56	45.00	1250.00	1.39	6.40	0.61	4.5
P5	0.83	8.82	48.47	813.00	1.55	11.50	0.61	4.5
P6	0.83	7.72	49.47	813.00	1.24	0.50	0.57	3.7
P7	0.82	8.70	41.15	751.87	1.51	8.74	0.58	4.2
P8	0.85	9.23	35.71	934.57	1.35	7.16	0.62	4.9

TABLE 3. Values obtained for parameters R_s, R_p, J_s, γ, illumination current density J_L, and charge generation rate G, with the Lambert W function

Polymer code	$R_s\,(\Omega/cm^2)$	$R_p\,(\Omega/cm^2)$	$J_s\,(mA/cm^2)$	γ	$J_L\,(mA/cm^2)$	$G\,(/cm^3\cdot s)\cdot 10^{23}$
P1	50.42	836.03	6.8	1.08	7.2	4.51
P2	105.40	1287.8	4.0	1.29	6.0	3.77
P3	53.29	1065.6	8.4	1.67	10.2	6.39
P3	45.10	1452.8	9.2	1.39	9.3	5.79
P4	48.63	1004.2	9.4	1.56	11.5	7.15
P5	49.62	927.1	8.0	1.24	8.5	5.33
P6	41.40	948.2	9.8	1.52	9.3	5.84
P7	35.91	1234.7	10.6	1.36	9.3	5.83

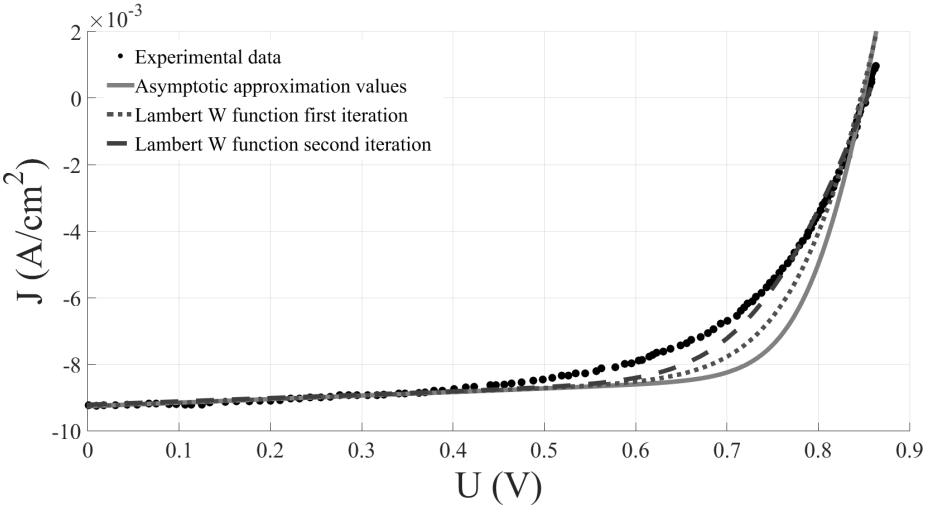

FIGURE 4. Plot of the experimental data and the fitting functions with the asymptotic and Lambert W methods

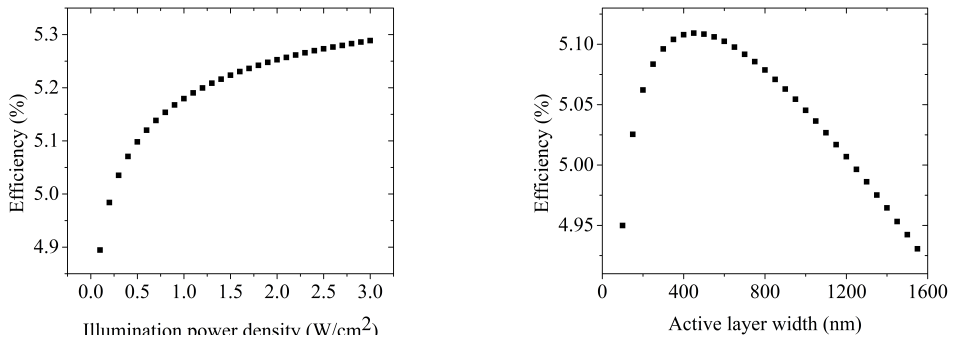

FIGURE 5. (A) Variation of the probe efficiency with illumination power density, and (B) Variation of the probe efficiency with the active layer width.

6. Conclusions

A theoretical characterization of several polymer-blend organic solar cells has been conducted. The mathematical methods used to calculate the circuit parameters were the asymptotic and the W Lambert function. After parameter estimation, for one sample, the parameters were used to fit the available experimental data of the current-voltage characteristic. The fittings show that the parameters extracted with the Lambert function are closer to the real values, due to the fact that they offer a better fit than the asymptotic-determined parameters. Furthermore, based on the calculated parameters, a classification between the different solar cell samples has been set up. Based on the results obtained for the fill-factor and the power conversion efficiency, it was concluded that the highest performing prototype is the one based on the $P(4)\text{-}T4-SiDT:PC_{71}BM\,(1:1)+2\%DIO$ on $MoO_3; Ca/Al$ polymer blend, which has yielded the highest fill-factor, $FF = 0.62$, and the highest efficiency, $PCE = 4.9\%$. This probe was subject of further studies, which consist of determining how the width L of the active layer influences the value of the power conversion efficiency of the cell in question. It has been shown that an optimal efficiency $PCE = 5.11\%$ is obtained for width $L = 500\ nm$.

Acknowledgements

Ana Bărar would like to acknowledge the financial support granted by the University "Politehnica" of Bucharest, in the form of a Ph. D. scholarship (Doctoral Contract No: SD04/07/2016).

REFERENCES

[1] *M. Carrasco-Orozco, W. C. Tsoi, M. O'Neill, M. P. Aldred, P. Vlachos and S. M. Kelly*, New photovoltaic concept: liquid-crystal solar cell using a nematic gel template, Advanced Materials,**13**(2006).

[2] *D. Mănăilă-Maximean, C. Roșu, O. Dănilă, D. Donescu, M. Ghiurea and F. Cotorobăi*, Electrical Field Induced Properties of Nematic Liquid Crystal/Copolymer Particles Composite, U. P. B. Scientific Bulletin Series A,**73**(2011).

[3] *N. Yamanaka, R. Kawano, W. Kubo, T. Kitamura, Y. Wada, M. Watanabe and S. Yanagida*, Ionic liquid crystal as a hole transport layer of dye-sensitized solar cells, Chem. Commun.,**73**(2011), 740-742 (DOI 10.1039/B417610C).

[4] *J. M. Gilli and S. Thiberge and D. Mănăilă-Maximean*, New aspect of the voltage/confinement ratio phase diagram for a confined homeotropic cholesteric, Molecular Crystals and Liquid Crystals,**1**(2004), 207-213.

[5] *S. Leng, L. H. Chan, J. Jing, J. Hu, R. M. Moustafa, R. M. van Horn, M. J. Graham, B. Sun, M. Zhu, K. Jeong, B. R. Kaafarani, W. Zhang, F. W. Harris and S. Z. D. Cheng*, From crystals to columnar liquid crystal phases: molecular design, synthesis and phase structure chracterization of a series of novel phenazines potentially useful in photovoltaic applications, Soft Matter, **6**(2010), 100-112.

[6] *C. Roșu, D. Mănăilă-Maximean and A. J. Paraskos*, Thermally Stimulated Depolarization Currents and Optical Transmissions Studies on A 3, 4-Dicyanothiophene-Based Bent-Rod Liquid Crystal, Modern Physics Letters B,**13**(2002), 473-483.

[7] *J. C. Hindson, B. Ulgut, R. M. Friend, N. C. Greenham, B. Norder, A. Kotlewski and T. J. Dingemans*, All-aromatic liquid crystal triphenylamine-based poly(azomethine)s as hole transport materials for optoelectronic applications, Journal of Materials Chemistry, **20**(2010), 937-944.

[8] *C. Roșu, D. Mănăilă-Maximean, S. Kundu, P. L. Almeida and O. Dănilă*, Perspectives on the electrically induced properties of electrospun cellulose/liquid crystal devices, Journal of Electrostatics,**69**(2011), 623-630.

[9] *Y. M. Yang, W. Chen, L. Dou, W. H. Chang, H. S. Duan, B. Bob, G. Li and Y. Yang*, High-performance multiple-donor bulk heterojunction solar cells, Nature Photonics,**9**(2015), 190-198.

[10] *D. Mănăilă-Maximean, C. Cârtoaje, O. Dănilă and D. Donescu*, Novel Colloidal System: magnetite-polymer Particles/Lyotropic Liquid Crystal Under Magnetic Field, Journal of Magnetism and Magnetic Materials,**438**(2017).

[11] *M. C. Scharber, D. M uhlbacher, M. Koppe, P. Denck, C. Waldauf, A. J. Heeger and C. J. Brabec*, Design Rules for Donors in Bulk Heterojunction Solar Cells - Toward 10% Energy-Conversion Efficiency, Journal of Magnetism and Magnetic Materials,**438**(2017).

[12] *D. Mănăilă-Maximean*, New grafted ferrite particles/liquid crystal composite under magnetic field, Journal of Magnetism and Magnetic Materials,**452**(2018), 343-348.

[13] *C. Winder and N. S. Sariciftci*, Low bandgap polymers for photon harvesting in bulk heterojunction solar cells, Journal of Materials Chemistry,**14**(2004), 1077-1086.

[14] *Y. Liu, J. Zhao, Z. Li, C. Mu, W. Ma, H. Hu, K. Jiang, H. Lin, H. Ade and H. Yan*, Aggregation and morphology control enables multiple cases of high-efficiency polymer solar cells, Nature Communications,**5**(2014).

[15] *D. Mănăilă-Maximean, O. Dănilă, P. L. Almeida and C. P. Ganea*, Electrical properties of a liquid crystal dispersed in an electrospun cellulose acetate network, Beilstein Journal of Nanotechnology,**9**(2018), 155-163.

[16] *M. W. Rowell, M. A. Topinka, M. D. McGehee, H. J. Prall, G. Dennler, N. S. Sariciftci, L. Hu and G. Gruner*, Organic solar cells with carbon nanotube network electrodes, Applied Physics Letters,**88**(2006).

[17] *C. Cîrtoaje and E. Petrescu*, Measurement of magnetic anisotropy of multiwalled carbon nanotubes in nematic host, Physica E: Low-dimensional Systems and Nanostructures,**84**(2016), 244-248.

[18] *A. du Pasquier, H. E. Unalan, A. Kanwal, S. Miller, M. Chhowalla*, Concudcting and transparent single-wall carbon nanotube electrodes for polymer-fullerene solar cells, Applied Physics Letters,**87**(2005).

[19] *C. Cîrtoaje, E. Petrescu, C. Stan and D. Creangă*, Ferromagnetic nanoparticles suspensions in twisted nematic, Physica E: Low-dimensional Systems and Nanostructures,**79**(2016), 38-43.

[20] *H. Hoppe and N. S. Sariciftici*, Organic solar cells: an overview, Journal of Material Research, **19**(2004), 1942-1945.

[21] *A. M. Bagher*, Comparison of organic solar cells and inorganic solar cells, International Journal of Renewable and Sustainable Energy,**3**(2014).

[22] *B. A. Gregg*, Excitonic solar cells, Journal of Physical Chemistry, **107**(2003), 4688-4698.

[23] *M. Bolognesi*, Organic bulk-heterojunction photovoltaic devices: materials, device architectures and interfacial processes, Universitat Rovira i Virgili (2013).

[24] *P. W urfel*, Physics of Solar Cells: From Principles to New Concepts, WILEY-VCH Velrag GmbH and Co. KGaA, Weinheim (2005)(ISBN 3-527-40428-7).

[25] *T. J. Savenjie*, Organic solar cells, Delft University of Technology, (2014).

[26] *A. Bărar, D. Mănăilă-Maximean, O. Dănilă, M. Vlădescu* , Parameter extraction of an organic solar cell using asymptotic estimation and Lambert W function, Proc. SPIE 10010, Advanced Topics in Optoelectronics, Microelectronics, and Nanotechnologies VIII, 1001034(2016),(DOI 10.1117/12.2253968).

[27] *T. Aernouts*, Organic bulk heterojunction solar cells - From single cell towards fully flexible photovoltaic module, Katholieke Universiteit Leuven, (2006).

[28] *M. R. Mitroi, V. Iancu, L. Fara and M. L. Ciurea*, Numerical analysis of J-V characteristics of a polymer solar cell, Progress in Photovoltaics, **19**(2011), 301-306 (DOI 10.1002/pip.1026).

[29] *G. del Pozo, B. Romero and B. Arrendondo*, Extraction of circuital parameters of organic solar cells using the exact solution based on Lambert W-function, Proc. SPIE, **8435**(2012),(DOI 10.1117/12.922461).

[30] *S. Yoo, B. Domercq and B. Kippelen*, Intensity-dependent equivalent circuit parameters of organic solar cells based on pentacene C_{60}, Journal of Applied Physics, **97**(2005).

[31] *K. Ishibashi, Y. Kimura and M. Niwano*, An extensively valid and stable method for derivation of all parameters of a solar cell from a single current-voltage characteristic, Journal of Applied Physics, **103**(2008).

[32] *R. M. Corless, G. H. Gonnet, D. E. G. Hare, D. J. Jeffrey and D. E. Knut*, On the Lambert W function, Advances in Computational Mathematics, **5**(1996), 329-359.

[33] *A. Jain and. A. Kapoor*, A new approach to study organic solar cell using Lambert W-function, Solar Energy Materials and Solar Cells, **86**(2005), 197-205.

[34] *M. R. Mitroi, V. Ninulescu and L. Fara*, Performance Optimization of Solar Cells Based on Heterojunction with Cu_2O: Numerical Analysis, Journal of Energy Engineering, **143**(2017).

[35] *M. S. Su, C. Y. Kuo, M. C. Yuan, U. Jeng, C. J. Su, K. H. Wei*, Improving device efficiency of polymer/fullerene bulk heterojunction solar cells through enhanced crystallinity and reduced grain boundaries induced by solvent additives, Advanced Materials, **23**(2011).

[36] *K. A. Vivek and G. D. Agrawal*, Organic solar cells: principles, mechanisms and recent developments, International Journal of Research in Engineering and Technology, **3**(2014).

[37] *J. J. Halls and R. H. Friend*, Organic photovoltaic devices, Clean Energy from Photovoltaics, Springer-Verlag, (2001).